ARTICLE

Typeset with jnst.cls <ver.2.1>

Perturbation theory for nuclear fuel depletion calculations with predictor-corrector method

Go Chiba[1]*

[1]*Hokkaido University, Kita-ku, Sapporo 060-8628, Japan*

The perturbation theory for nuclear fuel depletion calculations with the predictor-corrector method is derived. This theory is implemented to a reactor physics code system CBZ, and the theory itself and its implementation are numerically verified. Sensitivities of nuclide number densities after fuel depletion with respect to nuclear data calculated with this theory are compared with reference sensitivities calculated by numerical differentiation, and good agreements are obtained. Importance of accurate angle integration on product of neutron flux and generalized adjoint neutron flux is also pointed out. Sensitivities in a 3×3 multicell system including a gadolinium-bearing fuel pin are calculated, and it is demonstrated that the derived theory yields accurate sensitivities even if coarse depletion time step division is adopted. The present work drastically increases the applicability of the depletion perturbation theory to actual problems.

Keywords: nuclear fuel depletion; depletion perturbation theory; predictor-corrector method

*Corresponding author. Email: go_chiba@eng.hokudai.ac.jp

1. Introduction

In the field of reactor physics, sensitivity and uncertainty (S/U) analyses for reactor physics (neutronics) parameters have been paid significant attentions in recent years. While there are a lot of uncertain numerical processes and fundamental data in prediction of reactor physics parameters, neutron-nuclide reaction data, that is the nuclear data, is one of dominant sources of uncertainty. So many efforts have been devoted to quantification of nuclear data-induced uncertainty of reactor physics parameters so far.

A lot of numerical procedures for S/U analyses have been proposed. They can be categorized into the adjoint-based procedure and the stochastic-based (random sampling-based) procedure. Both of these procedures possess their own specific features. One of the specific features of the adjoint-based procedure is that it uses sensitivity profile (or sensitivity) of reactor physics parameters with respect to nuclear data. Sensitivity is quite convenient and useful quantity to understand physical process and to specify nuclear data which are dominant uncertainty source of predicted reactor physics parameters. Sensitivity is generally calculated by the well-established (generalized) perturbation theory.

S/U analyses for quantities related to nuclear fuel depletion have been also carried out by several researchers. Those quantities such as nuclide number densities after fuel depletion are quite important in many fields of nuclear engineering, such as reactor core design, safety analyses, and spent fuel storage, transportation, reprocessing and long-term disposal. The perturbation theory for these quantities, the *depletion perturbation theory*, was established initially for only neutron field by Gandini[1], and it was extended to coupled neutron/nuclide field by Williams[2]. These seminal and excellent works have been further extended and applied to fast reactor design calculations[3, 4]. Recently, the present author has implemented the depletion perturbation theory for multicell systems consisting of different types of light water reactors (LWRs) fuel pins to their own code system[5]. In order to apply the depletion perturbation theory to actual LWR fuel assem-

bly calculations, burnable absorber materials which are introduced to suppress positive reactivity at the beginning of depletion should be treated. It has been widely recognized that time discretization errors are significant in fuel depletion calculations of actual LWR fuel assemblies due to strong neutron absorptions of these absorber materials and significant change of their number densities. To overcome this difficulty, the predictor-corrector (PC) method is generally employed[6]. Thus the depletion perturbation theory which can be applied to depletion calculations with the PC method should be established.

In the present paper, we derive the perturbation theory for depletion calculations with the PC method, and implement it to our own code system. Verification tests are also carried out.

The present paper is organized as follows. Section 2 overviews the original depletion perturbation theory and describes newly derived depletion perturbation theory suited to the PC method. An important issue in numerical procedure, which is specific in calculating systems including strong neutron absorbers, and actual implementations are also described. Numerical results of verification tests and investigation on time discretization errors in sensitivities calculated with the derived theory are shown in Section 3, and Section 4 provides conclusion and future perspective.

2. Theory and implementation

2.1. Perturbation theory for depletion calculations without predictor-corrector method

In this subsection, the perturbation theory for depletion calculations without the PC method is described. For simplicity, systems consisting of a single depletion region are considered. Sub-step division of depletion time step for accurate neutron flux normalization is also neglected. The depletion perturbation theory for systems consisting of several depletion regions with sub-step division of depletion step are described in detail in our

previous paper[5].

Unnormalized neutron flux at time step i, Φ_i, is defined as solution to the following neutron transport equation:

$$\mathbf{B}_i\Phi_i = \left(\mathbf{A}_i - \frac{1}{k_{\text{eff},i}}\mathbf{F}_i\right)\Phi_i = 0, \tag{1}$$

where k_{eff} is the effective neutron multiplication factor, and $\mathbf{A}$ and $\mathbf{F}$ are operators for neutron loss and production, respectively. Neutron flux is normalized so as to preserve the following normalization condition:

$$\mathbf{G}_i\phi_i = \mathbf{G}_i\Phi_i f_i = P, \tag{2}$$

where $\mathbf{G}$ is an operator for the normalization, f is a normalization factor, and P is a quantity for the normalization such as reactor thermal power. We denote spatially-averaged energy-integrated value for Φ_i, that is spatially-averaged total neutron flux, in a depletion region as $\tilde{\Phi}_i$, which is defined as

$$\tilde{\Phi}_i = \frac{\int dE \int d\mathbf{r}\Phi_i(\mathbf{r}, E)}{\int d\mathbf{r}}, \tag{3}$$

where spatial integration is carried out over the depletion region. Similar quantity for the normalized neutron flux is also defined as

$$\tilde{\phi}_i = f_i\tilde{\Phi}_i. \tag{4}$$

The nuclide depletion equation during the time step i is described as follows:

$$\frac{d\mathbf{N}(t)}{dt} = \mathbf{M}_i\mathbf{N}(t), \quad (t_i \leq t < t_{i+1}), \tag{5}$$

where $\mathbf{N}(t)$ is a nuclide number density vector at t. A fuel depletion matrix at step i, $\mathbf{M}_i$, is decomposed as follows:

$$\mathbf{M}_i = \mathbf{M}_\lambda + \mathbf{M}_{\phi,i}\tilde{\phi}_i = \mathbf{M}_\lambda + \mathbf{M}_{\phi,i}f_i\tilde{\Phi}_i, \tag{6}$$

where $\mathbf{M}_\lambda$ and $\mathbf{M}_{\phi,i}$ are fuel depletion matrix components for radioactive decay and neutron-nuclide reaction. Note that entries of $\mathbf{M}_{\phi,i}$ consist of one-group (or energy-

averaged) cross sections.

A vector $\mathbf{w}(t)$, whose size is the same as that of $\mathbf{N}$, is multiplied to both sides of Eq. (5), both the sides are integrated over $[t_i, t_{i+1}]$, and then the following equations are derived.

$$\begin{aligned}
\int_{t_i}^{t_{i+1}} \mathbf{w}^T \frac{d\mathbf{N}}{dt} dt &= \int_{t_i}^{t_{i+1}} \mathbf{w}^T \mathbf{M}_i \mathbf{N} dt, \\
\left[\mathbf{w}^T \mathbf{N}\right]_{t_i}^{t_{i+1}} &= \int_{t_i}^{t_{i+1}} \frac{d\mathbf{w}^T}{dt} \mathbf{N} dt + \int_{t_i}^{t_{i+1}} \mathbf{w}^T \mathbf{M}_i \mathbf{N} dt, \\
\mathbf{w}^T(t_{i+1})\mathbf{N}(t_{i+1}) &= \mathbf{w}^T(t_i)\mathbf{N}(t_i) + \int_{t_i}^{t_{i+1}} \frac{d\mathbf{w}^T}{dt} \mathbf{N} dt + \int_{t_i}^{t_{i+1}} \mathbf{w}^T \mathbf{M}_i \mathbf{N} dt, \qquad (7)
\end{aligned}$$

where the superscript T is for transposition of matrices and vectors. Note that dependence of $\mathbf{N}$ and $\mathbf{w}$ on t is omitted here. By taking derivative of both the sides by nuclear data σ, the following equation is obtained:

$$\mathbf{w}^T(t_{i+1}) \frac{d\mathbf{N}(t_{i+1})}{d\sigma} = \mathbf{w}^T(t_i) \frac{d\mathbf{N}(t_i)}{d\sigma} + I_i, \qquad (8)$$

where

$$I_i = \int_{t_i}^{t_{i+1}} \frac{d\mathbf{w}^T}{dt} \frac{d\mathbf{N}}{d\sigma} dt + \int_{t_i}^{t_{i+1}} \mathbf{w}^T \frac{d\mathbf{M}_i}{d\sigma} \mathbf{N} dt + \int_{t_i}^{t_{i+1}} \mathbf{w}^T \mathbf{M}_i \frac{d\mathbf{N}}{d\sigma} dt. \qquad (9)$$

When $\mathbf{w}(t_{i+1}) = \mathbf{e}_j$, where $\mathbf{e}_j$ is a vector in which the jth entry is unity and others are zero, Eq. (8) is rewritten as

$$\frac{dN_j(t_{i+1})}{d\sigma} = \mathbf{w}^T(t_i) \frac{d\mathbf{N}(t_i)}{d\sigma} + I_i. \qquad (10)$$

Similarly the following equation on the derivative $\dfrac{d\mathbf{N}}{d\sigma}$ at $t = t_i$ can be obtained:

$$\mathbf{w}^T(t_i) \frac{d\mathbf{N}(t_i)}{d\sigma} = \mathbf{w}^T(t_{i-1}) \frac{d\mathbf{N}(t_{i-1})}{d\sigma} + I_{i-1}. \qquad (11)$$

If initial condition of the number density vector is defined at $t = t_1$, the following equation is derived:

$$\frac{dN_j(t_{i+1})}{d\sigma} = \mathbf{w}^T(t_1) \frac{d\mathbf{N}(t_1)}{d\sigma} + \sum_{j=1}^{i} I_j = \sum_{j=1}^{i} I_j, \qquad (12)$$

since $\dfrac{d\mathbf{N}(t_1)}{d\sigma} = 0$.

In the following, let us consider the integral term I_i defined in Eq. (9).

The first and third terms in the right hand side (RHS) of Eq. (9) disappear if the vector $\mathbf{w}$ is properly defined as described later. The second term can be rewritten as

$$\int_{t_i}^{t_{i+1}} \mathbf{w}^T \frac{d\mathbf{M}_i}{d\sigma}\mathbf{N}dt = \int_{t_i}^{t_{i+1}} \mathbf{w}^T \frac{\partial \mathbf{M}_i}{\partial \sigma}\mathbf{N}dt + \sum_g \frac{d\tilde{\Phi}_{i,g}}{d\sigma}\int_{t_i}^{t_{i+1}} \mathbf{w}^T \frac{\partial \mathbf{M}_i}{\partial \tilde{\Phi}_{i,g}}\mathbf{N}dt + \int_{t_i}^{t_{i+1}} \mathbf{w}^T \frac{df_i}{d\sigma}\frac{\partial \mathbf{M}_i}{\partial f_i}\mathbf{N}dt, \tag{13}$$

where $\tilde{\Phi}_{i,g}$ is spatially-averaged neutron flux of group g in the depletion region. The first term in RHS of Eq. (13) corresponds to direct effect of nuclear data to fuel depletion matrix, and partial derivative $\dfrac{\partial \mathbf{M}_i}{\partial \sigma}$ in this term can be easily calculated. The second and third terms correspond to indirect effects of nuclear data to fuel depletion matrix via neutron flux spatial and energy distributions and via neutron flux normalization factors, respectively.

Integral of the second term in RHS of Eq. (13) can be rewritten as

$$\int_{t_i}^{t_{i+1}} \mathbf{w}^T \frac{\partial \mathbf{M}_i}{\partial \tilde{\Phi}_{i,g}}\mathbf{N}dt = \int_{t_i}^{t_{i+1}} \mathbf{w}^T \frac{\partial \left(\mathbf{M}_{\phi,i}\tilde{\Phi}_i f_i\right)}{\partial \tilde{\Phi}_{i,g}}\mathbf{N}dt = f_i \int_{t_i}^{t_{i+1}} \mathbf{w}^T \mathbf{M}_{\phi,i,g}\mathbf{N}dt, \tag{14}$$

where

$$\mathbf{M}_{\phi,i,g} = \frac{\partial \left(\mathbf{M}_{\phi,i}\tilde{\Phi}_i\right)}{\partial \tilde{\Phi}_{i,g}}. \tag{15}$$

Since entries of the matrix $\mathbf{M}_{\phi,i}\tilde{\Phi}_i$ are reaction rates, entries of the matrix $\mathbf{M}_{\phi,i,g}$ are non-zero only if these are related to cross sections of group g.

Next, let us consider the third term in RHS of Eq. (13). By differentiating Eq. (2) by σ, the following equation can be derived:

$$\frac{df_i}{d\sigma}\frac{P}{f_i} + f_i\frac{d\mathbf{G}_i}{d\sigma}\Phi_i + f_i\mathbf{G}_i\frac{d\Phi_i}{d\sigma} = 0. \tag{16}$$

In the present paper, we assume

$$\frac{d\mathbf{G}_i}{d\sigma} = 0, \tag{17}$$

for simplicity. Then we can obtain

$$\frac{df_i}{d\sigma} = -\frac{f_i^2}{P}\mathbf{G}_i\frac{d\Phi_i}{d\sigma}. \tag{18}$$

With Eq.(18), the third term in RHS of Eq. (13) can be rewritten as

$$\begin{aligned}\int_{t_i}^{t_{i+1}} \mathbf{w}^T \frac{df_i}{d\sigma}\frac{\partial \mathbf{M}_i}{\partial f_i}\mathbf{N}dt &= \frac{df_i}{d\sigma}\int_{t_i}^{t_{i+1}} \mathbf{w}^T\left(\mathbf{M}_{\phi,i}\tilde{\Phi}_i\right)\mathbf{N}dt \\ &= -\frac{f_i^2}{P}\mathbf{G}_i\frac{d\Phi_i}{d\sigma}\int_{t_i}^{t_{i+1}} \mathbf{w}^T\left(\mathbf{M}_{\phi,i}\tilde{\Phi}_i\right)\mathbf{N}dt = -f_i P_i^\dagger \mathbf{G}_i\frac{d\Phi_i}{d\sigma},\end{aligned} \tag{19}$$

where

$$P_i^\dagger = \frac{\displaystyle\int_{t_i}^{t_{i+1}} \mathbf{w}^T\left(\mathbf{M}_{\phi,i}\tilde{\Phi}_i f_i\right)\mathbf{N}dt}{P}. \tag{20}$$

Also if we write

$$\mathbf{G}_i\Phi_i = V\sum_g G_{i,g}\tilde{\Phi}_{i,g}, \tag{21}$$

the third term in RHS of Eq. (13) can be written as

$$\int_{t_i}^{t_{i+1}} \mathbf{w}^T \frac{df_i}{d\sigma}\frac{\partial \mathbf{M}_i}{\partial f_i}\mathbf{N}dt = -f_i P_i^\dagger V\sum_g G_{i,g}\frac{d\tilde{\Phi}_{i,g}}{d\sigma}. \tag{22}$$

Note that V is volume of the depletion region.

With Eqs. (13), (14) and (22), the second term in RHS of Eq. (9) can be rewritten as

$$\begin{aligned}&\int_{t_i}^{t_{i+1}} \mathbf{w}^T \frac{d\mathbf{M}_i}{d\sigma}\mathbf{N}dt \\ &\quad= \int_{t_i}^{t_{i+1}} \mathbf{w}^T \frac{\partial \mathbf{M}_i}{\partial \sigma}\mathbf{N}dt + \sum_g \frac{d\tilde{\Phi}_{i,g}}{d\sigma}\left\{\left(f_i\int_{t_i}^{t_{i+1}} \mathbf{w}^T\mathbf{M}_{\phi,i,g}\mathbf{N}dt - VG_{i,g}f_iP_i^\dagger\right)\right\}.\end{aligned} \tag{23}$$

Next, let us consider the term $\dfrac{d\tilde{\Phi}_{i,g}}{d\sigma}$ in RHS of Eq. (23). By differentiating both sides of the neutron transport Eq. (1) by σ, we can obtain

$$\left(\frac{\partial \mathbf{B}_i}{\partial \sigma} + \frac{\partial \mathbf{B}_i}{\partial \mathbf{N}^T(t_i)}\frac{d\mathbf{N}(t_i)}{d\sigma}\right)\Phi_i + \mathbf{B}_i\frac{d\Phi_i}{d\sigma} = 0. \tag{24}$$

At this point the following generalized adjoint equation to Eq. (1) is defined:

$$\mathbf{B}_i^\dagger\Gamma_i^\dagger = S_i^\dagger. \tag{25}$$

The superscript † is used to denote adjoint operator and quantity. Boundary conditions for $\Gamma_i^\dagger$ should be properly chosen in accordance with those for Φ_i. The generalized adjoint neutron flux $\Gamma_i^\dagger$ is multiplied to both sides of Eq. (24) and both the sides are integrated over whole phase space. Then the following equation is derived:

$$\begin{aligned}
&\left\langle \Gamma_i^\dagger, \frac{\partial \mathbf{B}_i}{\partial \sigma}\Phi_i \right\rangle + \frac{d\mathbf{N}^T(t_i)}{d\sigma}\left\langle \Gamma_i^\dagger, \frac{\partial \mathbf{B}_i}{\partial \mathbf{N}(t_i)}\Phi_i \right\rangle + \left\langle \Gamma_i^\dagger, \mathbf{B}_i\frac{d\Phi_i}{d\sigma} \right\rangle \\
&= \left\langle \Gamma_i^\dagger, \frac{\partial \mathbf{B}_i}{\partial \sigma}\Phi_i \right\rangle + \frac{d\mathbf{N}^T(t_i)}{d\sigma}\left\langle \Gamma_i^\dagger, \frac{\partial \mathbf{B}_i}{\partial \mathbf{N}(t_i)}\Phi_i \right\rangle + \left\langle \frac{d\Phi_i}{d\sigma}, \mathbf{B}_i^\dagger\Gamma_i^\dagger \right\rangle \\
&= \left\langle \Gamma_i^\dagger, \frac{\partial \mathbf{B}_i}{\partial \sigma}\Phi_i \right\rangle + \frac{d\mathbf{N}^T(t_i)}{d\sigma}\left\langle \Gamma_i^\dagger, \frac{\partial \mathbf{B}_i}{\partial \mathbf{N}(t_i)}\Phi_i \right\rangle + \left\langle \frac{d\Phi_i}{d\sigma}S_i^\dagger \right\rangle = 0, \qquad (26)
\end{aligned}$$

where the brackets $\langle\rangle$ denote integration over whole phase space. If the source $S_i^\dagger$ is defined as spatially flat over the depletion region, the third term of Eq. (26) can be written as

$$\left\langle \frac{d\Phi_i}{d\sigma}S_i^\dagger \right\rangle = \sum_g S_{i,g}^\dagger \frac{d\tilde{\Phi}_{i,g}}{d\sigma}V. \qquad (27)$$

If we define the source $S_i^\dagger$ as

$$S_{i,g}^\dagger = -\frac{1}{V}\left(f_i \int_{t_i}^{t_{i+1}} \mathbf{w}^T \mathbf{M}_{\phi,i,g}\mathbf{N}dt - VG_{i,g}f_i P_i^\dagger \right), \qquad (28)$$

the second term in RHS of Eq. (23) can be written as

$$\sum_g \frac{d\tilde{\Phi}_{i,g}}{d\sigma}\left(f_i \int_{t_i}^{t_{i+1}} \mathbf{w}^T \mathbf{M}_{\phi,i,g}\mathbf{N}dt - VG_{i,g}f_i P_i^\dagger \right) = \left\langle \Gamma_i^\dagger, \frac{\partial \mathbf{B}_i}{\partial \sigma}\Phi_i \right\rangle + \frac{d\mathbf{N}^T(t_i)}{d\sigma}\left\langle \Gamma_i^\dagger, \frac{\partial \mathbf{B}_i}{\partial \mathbf{N}(t_i)}\Phi_i \right\rangle. \qquad (29)$$

It is important to note that the source $S_i^\dagger$ is orthogonal to the solution to the neutron transport Eq. (1), Φ_i, and that the Fredholm alternative theorem guarantees non-zero solutions to Eq. (25).

Finally the integral term I_i can be written as

$$\begin{aligned}
I_i = &\int_{t_i}^{t_{i+1}} \frac{d\mathbf{w}^T}{dt}\frac{d\mathbf{N}}{d\sigma}dt + \int_{t_i}^{t_{i+1}} \mathbf{w}^T\mathbf{M}_i\frac{d\mathbf{N}}{d\sigma}dt \\
&+ \int_{t_i}^{t_{i+1}} \mathbf{w}^T\frac{\partial \mathbf{M}_i}{\partial \sigma}\mathbf{N}dt + \left\langle \Gamma_i^\dagger, \frac{\partial \mathbf{B}_i}{\partial \sigma}\Phi_i \right\rangle + \frac{d\mathbf{N}^T(t_i)}{d\sigma}\left\langle \Gamma_i^\dagger, \frac{\partial \mathbf{B}_i}{\partial \mathbf{N}(t_i)}\Phi_i \right\rangle. \qquad (30)
\end{aligned}$$

The first, second and fifth terms in RHS of Eq. (30) which include the derivative $\frac{d\mathbf{N}}{d\sigma}$ disappear if $\mathbf{w}$ is defined as follows. Since the fifth term in RHS of Eq. (30) can be written

as

$$\int_{t_i}^{t_{i+1}} \delta(t-t_i) \frac{d\mathbf{N}^T(t)}{d\sigma} \left\langle \Gamma_i^\dagger, \frac{\partial \mathbf{B}_i}{\partial \mathbf{N}(t_i)} \Phi_i \right\rangle dt, \tag{31}$$

we define the following equation of $\mathbf{w}$ in $[t_i, t_{i+1}]$:

$$\frac{d\mathbf{w}(t)}{dt} + {\mathbf{M}_i}^T \mathbf{w}(t) + \left\langle \Gamma_i^\dagger, \frac{\partial \mathbf{B}_i}{\partial \mathbf{N}(t_i)} \Phi_i \right\rangle \delta(t-t_i) = 0. \tag{32}$$

This equation can be solved backward with the final condition for $\mathbf{w}(t_{i+1})$. This equation suggests that discontinuous change is given to $\mathbf{w}$ at the beginning of step, $t = t_i$. This is what is called the *jump condition*.

By virtue of the above definition of $\mathbf{w}$, representation of the integral term I_i is simplified into

$$I_i = \int_{t_i}^{t_{i+1}} \mathbf{w}^T \frac{\partial \mathbf{M}_i}{\partial \sigma} \mathbf{N} dt + \left\langle \Gamma_i^\dagger, \frac{\partial \mathbf{B}_i}{\partial \sigma} \Phi_i \right\rangle. \tag{33}$$

2.2. Perturbation theory for depletion calculations with predictor-corrector method

The perturbation theory for depletion calculations with the PC method are described in this subsection. We will describe the theory for the weighted PC method for more generality[7].

At the first stage of the PC method, predictor calculation is carried out. This is the exactly same as depletion calculation without the PC method. In the following, nuclide number density vector at $t = t_{i+1}$ obtained in the predictor calculation for a time step i is denoted to as $\mathbf{N}^p(t_{i+1})$. At the next stage, corrector calculation is carried out. In the corrector calculation, neutron flux distribution Φ_i^c is recalculated with $\mathbf{N}^p(t_{i+1})$ as follows:

$$\mathbf{B}_i^c(\mathbf{N}^p(t_{i+1}))\Phi_i^c = 0, \tag{34}$$

and this neutron flux is normalized as

$$\mathbf{G}_i \phi_i^c = \mathbf{G}_i \Phi_i^c f_i^c = P. \tag{35}$$

With the neutron flux ϕ_i^c and one-group cross sections calculated from ϕ_i^c, nuclide depletion calculation is carried out with the following equation with initial condition, $\mathbf{N}^c(t_i) = \mathbf{N}(t_i)$:

$$\frac{d\mathbf{N}^c(t)}{dt} = \mathbf{M}_i^c \mathbf{N}^c(t), \quad (t_i \leq t < t_{i+1}). \tag{36}$$

By solving Eq. (36), $\mathbf{N}^c(t_{i+1})$ can be obtained. There are two variants to obtain number density at $t = t_{i+1}$, $\mathbf{N}(t_{i+1})$, from $\mathbf{N}^p(t_{i+1})$ and $\mathbf{N}^c(t_{i+1})$ in the weighted PC method. The first one is weighted-averaging as

$$\mathbf{N}(t_{i+1}) = \omega_p \mathbf{N}^p(t_{i+1}) + \omega_c \mathbf{N}^c(t_{i+1}), \tag{37}$$

and the second one is weighted-logarithmic averaging as

$$\ln \mathbf{N}(t_{i+1}) = \omega_p \ln \mathbf{N}^p(t_{i+1}) + \omega_c \ln \mathbf{N}^c(t_{i+1}). \tag{38}$$

These weights, ω_p and ω_c, should be positive and sum of them should be unity. The latter averaging is consistent with weighted-averaging on reaction rates. In the following the weighted PC method with the weighted-averaging shown in Eq. (37) is considered because of its simplicity.

By differentiating both the sides of Eq. (37) by σ, the following equation is obtained:

$$\frac{dN_j(t_{i+1})}{d\sigma} = \omega_p \frac{dN_j^p(t_{i+1})}{d\sigma} + \omega_c \frac{dN_j^c(t_{i+1})}{d\sigma}. \tag{39}$$

Similar to Eq. (10), $\frac{dN_j^p(t_{i+1})}{d\sigma}$ and $\frac{dN_j^c(t_{i+1})}{d\sigma}$ are written as follows:

$$\frac{dN_j^p(t_{i+1})}{d\sigma} = \mathbf{w}^{pT}(t_i) \frac{d\mathbf{N}^p(t_i)}{d\sigma} + I_i^p = \mathbf{w}^{pT}(t_i) \frac{d\mathbf{N}(t_i)}{d\sigma} + I_i^p, \tag{40}$$

$$\frac{dN_j^c(t_{i+1})}{d\sigma} = \mathbf{w}^{cT}(t_i) \frac{d\mathbf{N}^c(t_i)}{d\sigma} + I_i^c = \mathbf{w}^{cT}(t_i) \frac{d\mathbf{N}(t_i)}{d\sigma} + I_i^c. \tag{41}$$

Note that for $\mathbf{w}^p$ and $\mathbf{w}^c$ the common final condition $\mathbf{w}^p(t_{i+1}) = \mathbf{w}^c(t_{i+1}) = \mathbf{e}_j$ are assigned. By inserting Eqs. (40) and (41) into Eq. (39), the following equation is obtained:

$$\begin{aligned} \frac{dN_j(t_{i+1})}{d\sigma} &= \left(\omega_p \mathbf{w}^{pT}(t_i) + \omega_c \mathbf{w}^{cT}(t_i)\right) \frac{d\mathbf{N}(t_i)}{d\sigma} + \omega_p I_i^p + \omega_c I_i^c \\ &= \tilde{\mathbf{w}}^T(t_i) \frac{d\mathbf{N}(t_i)}{d\sigma} + \omega_p I_i^p + \omega_c I_i^c, \end{aligned} \tag{42}$$

where

$$\tilde{\mathbf{w}}(t_i) = \omega_p \mathbf{w}^p(t_i) + \omega_c \mathbf{w}^c(t_i). \tag{43}$$

This means that $\tilde{\mathbf{w}}$ is calculated from $\mathbf{w}^p$ and $\mathbf{w}^c$ at the beginning of time step and this is used as the final condition of the preceding time step in adjoint number density calculations. If initial condition of the number density vector is defined at $t = t_1$, the following equation is derived:

$$\frac{dN_j(t_{i+1})}{d\sigma} = \tilde{\mathbf{w}}^T(t_1)\frac{d\mathbf{N}(t_1)}{d\sigma} + \sum_{j=1}^{i}\left(\omega_p I_j^p + \omega_c I_j^c\right) = \sum_{j=1}^{i}\left(\omega_p I_j^p + \omega_c I_j^c\right). \tag{44}$$

Next numerical procedure to obtain the integral terms I^p and I^c is described.

The term I^p can be written in the following equation:

$$\begin{aligned} I_i^p = &\int_{t_i}^{t_{i+1}} \frac{d\mathbf{w}^{pT}}{dt}\frac{d\mathbf{N}^p}{d\sigma}dt + \int_{t_i}^{t_{i+1}} \mathbf{w}^{pT}\mathbf{M}_i^p\frac{d\mathbf{N}^p}{d\sigma}dt \\ &+ \int_{t_i}^{t_{i+1}} \mathbf{w}^{pT}\frac{\partial \mathbf{M}_i^p}{\partial\sigma}\mathbf{N}^p dt + \left\langle \Gamma_i^{\dagger,p}, \frac{\partial \mathbf{B}_i^p}{\partial\sigma}\Phi_i^p \right\rangle + \frac{d\mathbf{N}^{pT}(t_i)}{d\sigma}\left\langle \Gamma_i^{\dagger,p}, \frac{\partial \mathbf{B}_i^p}{\partial \mathbf{N}^p(t_i)}\Phi_i^p \right\rangle. \end{aligned} \tag{45}$$

This is the exactly same as Eq. (30), but the superscript p is used to distinguish quantities in the predictor calculation from those in the corrector calculation. On the other hand, one has to take care in calculating I^c since the neutron transport operator $\mathbf{B}$ in the corrector calculation depends on not $\mathbf{N}(t_i)$ but $\mathbf{N}^p(t_{i+1})$. The term I^c can be written as

$$\begin{aligned} I_i^c = &\int_{t_i}^{t_{i+1}} \frac{d\mathbf{w}^{cT}}{dt}\frac{d\mathbf{N}^c}{d\sigma}dt + \int_{t_i}^{t_{i+1}} \mathbf{w}^{cT}\mathbf{M}_i^c\frac{d\mathbf{N}^c}{d\sigma}dt \\ &+ \int_{t_i}^{t_{i+1}} \mathbf{w}^{cT}\frac{\partial \mathbf{M}_i^c}{\partial\sigma}\mathbf{N}^c dt + \left\langle \Gamma_i^{\dagger,c}, \frac{\partial \mathbf{B}_i^c}{\partial\sigma}\Phi_i^c \right\rangle + \frac{d\mathbf{N}^{pT}(t_{i+1})}{d\sigma}\left\langle \Gamma_i^{\dagger,c}, \frac{\partial \mathbf{B}_i^c}{\partial \mathbf{N}^p(t_{i+1})}\Phi_i^c \right\rangle. \end{aligned} \tag{46}$$

Thus sum of the second and third terms in Eq. (42) is rewritten as

$$\omega_p I_i^p + \omega_c I_i^c = \omega_p \bar{I}_i^p + \omega_c \bar{I}_i^c, \tag{47}$$

where

$$\bar{I}_i^p = \int_{t_i}^{t_{i+1}} \frac{d\mathbf{w}^{pT}}{dt}\frac{d\mathbf{N}^p}{d\sigma}dt + \int_{t_i}^{t_{i+1}} \mathbf{w}^{pT}\mathbf{M}_i^p\frac{d\mathbf{N}^p}{d\sigma}dt + \int_{t_i}^{t_{i+1}} \mathbf{w}^{pT}\frac{\partial \mathbf{M}_i^p}{\partial\sigma}\mathbf{N}^p dt$$

$$+\left\langle \Gamma_i^{\dagger,p}, \frac{\partial \mathbf{B}_i^p}{\partial \sigma}\Phi_i^p \right\rangle + \frac{d\mathbf{N}^{pT}(t_i)}{d\sigma}\left\langle \Gamma_i^{\dagger,p}, \frac{\partial \mathbf{B}_i^p}{\partial \mathbf{N}^p(t_i)}\Phi_i^p \right\rangle + \frac{\omega_c}{\omega_p}\frac{d\mathbf{N}^{pT}(t_{i+1})}{d\sigma}\left\langle \Gamma_i^{\dagger,c}, \frac{\partial \mathbf{B}_i^c}{\partial \mathbf{N}^p(t_{i+1})}\Phi_i^c \right\rangle, \tag{48}$$

$$\bar{I}_i^c = \int_{t_i}^{t_{i+1}} \frac{d\mathbf{w}^{cT}}{dt}\frac{d\mathbf{N}^c}{d\sigma}dt + \int_{t_i}^{t_{i+1}} \mathbf{w}^{cT}\mathbf{M}_i^c\frac{d\mathbf{N}^c}{d\sigma}dt + \int_{t_i}^{t_{i+1}} \mathbf{w}^{cT}\frac{\partial \mathbf{M}_i^c}{\partial \sigma}\mathbf{N}^c dt + \left\langle \Gamma_i^{\dagger,c}, \frac{\partial \mathbf{B}_i^c}{\partial \sigma}\Phi_i^c \right\rangle. \tag{49}$$

We finally define the following equations for $\mathbf{w}^c$ and $\mathbf{w}^p$ in $[t_i, t_{i+1}]$:

$$\frac{d\mathbf{w}^p(t)}{dt} + \mathbf{M}_i^{pT}\mathbf{w}^p(t) + \left\langle \Gamma_i^{\dagger,p}, \frac{\partial \mathbf{B}_i^p}{\partial \mathbf{N}^p(t_i)}\Phi_i^p \right\rangle \delta(t-t_i) + \frac{\omega_c}{\omega_p}\left\langle \Gamma_i^{\dagger,c}, \frac{\partial \mathbf{B}_i^c}{\partial \mathbf{N}^p(t_{i+1})}\Phi_i^c \right\rangle \delta(t-t_{i+1}) = 0, \tag{50}$$

$$\frac{d\mathbf{w}^c(t)}{dt} + \mathbf{M}_i^{cT}\mathbf{w}^c(t) = 0. \tag{51}$$

This means that the jump condition is adopted at the beginning and end of each time step in the predictor calculation, and is not adopted in the corrector calculation. Finally the integral terms I^p and I^c are calculated as

$$\bar{I}_i^p = \int_{t_i}^{t_{i+1}} \mathbf{w}^{pT}\frac{\partial \mathbf{M}_i^p}{\partial \sigma}\mathbf{N}^p dt + \left\langle \Gamma_i^{\dagger,p}, \frac{\partial \mathbf{B}_i^p}{\partial \sigma}\Phi_i^p \right\rangle, \tag{52}$$

$$\bar{I}_i^c = \int_{t_i}^{t_{i+1}} \mathbf{w}^{cT}\frac{\partial \mathbf{M}_i^c}{\partial \sigma}\mathbf{N}^c dt + \left\langle \Gamma_i^{\dagger,c}, \frac{\partial \mathbf{B}_i^c}{\partial \sigma}\Phi_i^c \right\rangle. \tag{53}$$

2.3. Angle integration of product of neutron flux and generalized adjoint neutron flux

In the preceding sections, angle dependence of neutron flux is not explicitly treated for simplicity. Rigorously speaking, integral calculations of product of neutron flux Φ and generalized adjoint neutron flux $\Gamma^\dagger$ on angle are required in neutron flux term calculations of sensitivities shown in Eqs. (33), (52) and (53).

A neutron flux term in sensitivity with explicit representation of integration is written as follows:

$$\left\langle \Gamma_i^\dagger, \frac{\partial \mathbf{B}_i}{\partial \sigma}\Phi_i \right\rangle = \sum_g \int \frac{\partial \mathbf{B}_i(\mathbf{r})}{\partial \sigma_g} d\mathbf{r} \int \Gamma_{i,g}^\dagger(\mathbf{r}, \mathbf{\Omega})\Phi_{i,g}(\mathbf{r}, \mathbf{\Omega}) d\mathbf{\Omega}, \tag{54}$$

where $\mathbf{\Omega}$ is denoted to as angle direction. If angular dependence of Φ and $\Gamma^{\dagger}$ is insignificant, one can introduce the following approximation to this integral calculation on angle:

$$\int \Gamma^{\dagger}_{i,g}(\mathbf{r},\mathbf{\Omega})\Phi_{i,g}(\mathbf{r},\mathbf{\Omega})d\mathbf{\Omega} \approx \frac{1}{4\pi}\hat{\Gamma}^{\dagger}_{i,g}(\mathbf{r})\hat{\Phi}_{i,g}(\mathbf{r}), \tag{55}$$

where

$$\hat{\Gamma}^{\dagger}_{i,g}(\mathbf{r}) = \int \Gamma^{\dagger}_{i,g}(\mathbf{r},\mathbf{\Omega})d\mathbf{\Omega}, \tag{56}$$

$$\hat{\Phi}_{i,g}(\mathbf{r}) = \int \Phi_{i,g}(\mathbf{r},\mathbf{\Omega})d\mathbf{\Omega}. \tag{57}$$

This approximation is referred to as an *isotropic approximation* in the present paper. In our previous study, we have introduced this approximation implicitly since the classical collision probability method, which cannot calculate angular neutron flux and angular generalized adjoint neutron flux, is employed. This was not mentioned in our previous paper. This approximation has not resulted in significant impacts on depletion sensitivity calculations for single pincell and multicell systems including different types of fuel (UO_2 and MOX) since calculated sensitivities have agreed well with references. Through the present study, however, it is found that this approximation resulted in significant errors in depletion sensitivities when systems including strong neutron absorber materials, such as gadolinium, are considered. In order to calculate angular neutron flux and angular generalized adjoint neutron flux, we apply a numerical module based on the method of characteristics to depletion sensitivity calculations instead of the collision probability method.

Note that the angle integration calculations are required also in treating discontinuous change in adjoint number densities at the beginning (and end) of depletion steps introduced by the jump condition, which are shown in Eqs. (32) and (50).

2.4. Implementation of new depletion perturbation theory to deterministic reactor physics code system CBZ

The depletion perturbation theory derived in the preceding section is implemented to CBZ, which is a general-purpose reactor physics deterministic code system under development at Hokkaido University. The CBZ code system has various modules to solve neutron diffusion and transport equations based on the collision probability method, the method of characteristics, the finite-volume method, the boundary element method and the discrete-ordinate method. CBZ has other modules for reactor physics calculations such as resonance self-shielding treatment, fuel depletion and uncertainty quantification. The CBZ code system realizes various functionalities related to reactor physics and particle transport through combinations of these modules. Numerical procedure for fuel depletion calculations with CBZ is briefly described below.

Resonance self-shielding calculations, *i.e.,* effective cross sections calculations, are carried out in a single pincell model with reflective boundary conditions with the advanced Bondarenko method[8]. A JENDL-4.0-based 107-group library is used. The resonance self-shielding calculations yield 107-group cross sections which are used in subsequent neutron flux and fuel depletion calculations.

Neutron flux and generalized adjoint neutron flux are calculated by the method of characteristics as described in the preceding section. A module based on the method of characteristics implemented to CBZ has been verified in our previous study[9].

Changes in nuclide number densities through fuel depletion are described by the depletion equation (5), and this equation can be solved by various numerical methods. The CBZ code system employs the matrix exponential method, and the Mini-Max Polynomial Approximation (MMPA) method is used to calculate the matrix exponential[10]. Capability of fuel depletion calculations for multicell systems including a LWR fuel assembly has been verified in our previous study[7]. The MMPA method has a specific feature of being

capable of calculating nuclide number densities at several time steps at once without any significant increases in computation time. This is quite favorable in the depletion perturbation theory which requires numerical integration calculations on time interval during which integrated parameters such as **N** and **w** are significantly dependent on time.

At present, this module can calculate sensitivities of nuclide number densities after fuel depletion to nuclear data. Extension of this capability to various neutronics parameters, such as neutron multiplication factor and spectral indices, can be easily realized[11].

3. Numerical results

3.1. Problem specification

In the present study, a 3×3 multicell system consisting of PWR-simulated UO_2 fuel pins with the reflective boundary conditions is considered. Geometric configuration of this system is shown in **Figure 1**.

[Figure 1 about here.]

Uranium-235 enrichment of the UO_2 fuel pins, denoted as pin 2 and pin3 in this figure, is 4.1 wt%. Geometric specification and initial nuclide number densities are taken from the reference[12]. At the center position of this system, a gadolinium-bearing UO_2 fuel pin, whose gadolinium concentration is 10 wt% and uranium-235 enrichment is 4.0 wt%, is located. This gadolinium-bearing pin is divided into eight ring-type regions, and nuclides depletion calculations are carried out in each region. On the other normal fuel pins (pin 2 and pin 3), a whole fuel pellet region is treated as one depletion region. In actual numerical calculations, a 1/8 portion of this system with the reflective boundary conditions is considered.

Sensitivities of nuclide number densities after two different depletion (9.6 GWD/t and 20.8 GWD/t) with respect to several cross sections are calculated. Neutron flux is normalized with constant line power of 179 W/cm per one fuel pin in average. A

nuclide depletion chain consisting of 138 fission product nuclides, which is optimized for light water reactor reactivity calculations[13], is employed. Length of one depletion step is 1.6 GWD/t while finer depletion steps are used at the beginning and end of the depletion. For example, in sensitivity calculations at depletion of 9.6 GWD/t, 10 depletion steps, whose lengths are 0.04, 0.36, 1.2, 1.6, 1.6, 1.6, 1.6, 1.2, 0.36 and 0.04 GWD/t, are assigned. The reason why fine depletion steps are assigned around the end of the depletion is to capture drastic change in adjoint number densities of nuclides with short half-life or strong neutron absorption. One depletion step is further divided into 20 sub-steps. For the weighted PC method, ω_p and ω_c are set to 0.4 and 0.6, respectively. Infinite neutron multiplication factors obtained with or without the PC method are shown in **Figure 2**. This result clearly shows necessity of special numerical treatments such as the PC method in depletion calculations of nuclear fuel systems including strong neutron absorber materials.

[Figure 2 about here.]

3.2. Verification of derived theory and its implementation against reference sensitivities

In order to verify newly derived theory for fuel depletion sensitivity calculations with the PC method, sensitivities calculated by this theory are compared with reference sensitivities, which are calculated by numerical differentiation in which 1% perturbation is given to each of nuclear data and change in response parameters is observed. Common numerical conditions are adopted to both the perturbation theory calculations and the reference calculations. First, sensitivities of gadolinium-157 number density in pin 1 after depletion with respect to several nuclear data are discussed. **Figure 3** shows sensitivities at peripheral region of pin 1 after depletion of 9.6 GWD/t. Sensitivities multiplied by 0.25 per lethargy are displayed in these figures because lethargy width of each energy group

above 1.8554 eV is 0.25 in the present calculations. Sensitivities calculated by the new theory are denoted to as "DPT" in this figure, and those calculated with the isotropic approximation are as "DPT(IA)". Although sensitivities calculated with the perturbation theory with the isotropic approximation do not agree with the references in specific energy groups of some cross sections, those calculated with the perturbation theory without the isotropic approximation agree well with the references. These results clearly show importance of the explicit angular representation of neutron flux and generalized adjoint neutron flux in the depletion perturbation theory calculations for specific problems.

[Figure 3 about here.]

Figure 4 shows sensitivities at center region of pin 1 after depletion of 20.8 GWD/t. Good agreements between results with the perturbation theory without the isotropic approximation and the references can be observed.

[Figure 4 about here.]

Reaction cross sections of strong neutron absorber nuclides such as gadolinium-155 and -157 might affect neutron flux spatial and energy distributions, so number densities in fuel pins surrounding gadolinium-bearing fuel pin are expected to be sensitive to these cross sections at a certain degree. **Figure 5** shows sensitivities of number densities of several nuclides at pin 2 after depletion of 20.8 GWD/t with respect to gadolinium-157 capture cross section. Not as expected, these sensitivities are generally small. Those calculated by the perturbation theory without the isotropic approximation agree well with the references.

[Figure 5 about here.]

Through the above comparisons, the newly derived depletion perturbation theory with the PC method and its implementation have been well verified.

3.3. Depletion time step division-dependence of sensitivities

The PC method makes it possible to perform accurate fuel depletion calculations even with coarse depletion time step division. Thus it is also expected that sensitivities of nuclide number densities after depletion can be accurately calculated by the PC method with coarse depletion step division. To confirm this, several sensitivities of nuclide number densities are calculated with the depletion perturbation theory with and without the PC method. Three different depletion step division schemes are prepared to observe effects of step division on calculated sensitivities; depletion step used in the preceding calculations is further divided into 1, 2 or 4.

Figure 6 shows sensitivities of gadolinium-157 number density at center region of pin 1 after depletion of 9.6 GWD/t with respect to uranium-235 fission cross section. In these figures, "Div.=4" corresponds to results obtained by calculations in which the reference depletion step is further divided to 4, for example. Slight dependence of sensitivities on depletion step division is observed in results obtained without the PC method, but this is not significant. Interestingly similar results are obtained in most sensitivities; this suggests that time discretization is not sensitive to sensitivities of nuclide number densities after depletion even in systems including strong neutron absorber materials.

[Figure 6 about here.]

In some sensitivities, however, significant effects of time discretization are observed. **Figures 7** and **8** show sensitivities of gadolinium-157 and -155 number densities at center region of pin 1 after depletion of 9.6 GWD/t with respect to uranium-238 capture and uranium-235 fission cross sections. In sensitivities obtained without the PC method, significant dependence on depletion step division is observed and convergence cannot be attained even with the finest step division. On the other hand, in sensitivities obtained with the PC method, the reference, which is the most coarse step division, provides satisfactory results. These results show necessity and importance of the depletion perturbation

theory with the PC method newly derived in the present study.

[Figure 7 about here.]

[Figure 8 about here.]

4. Conclusion and future perspective

The perturbation theory for nuclear fuel depletion calculations with the PC method has been derived. This theory has been implemented to a reactor physics code system CBZ, and the theory itself and its implementation have been numerically verified. Sensitivities of nuclide number densities after fuel depletion calculated with the derived theory have been compared with reference sensitivities calculated by numerical differentiation, and good agreement has been obtained. During the course of these comparisons, importance of accurate angular integration of product of neutron flux and generalized adjoint neutron flux has been pointed out. Sensitivities in a 3×3 multicell system including gadolinium-bearing fuel pin have been calculated, and it has been demonstrated that the derived depletion perturbation theory with the PC method yields accurate sensitivities with negligible time discerization error even if coarse time step division is adopted. The present work drastically increases the applicability of the depletion perturbation theory to actual problems.

As future works, we will apply this new capability of CBZ to uncertainty quantification and its reduction of reactivity during fuel depletion of actual LWR fuel assemblies.

Acknowledgement

This work is supported by the secretariat of the nuclear regulation authority of Japan.

References

[1] Gandini A. A method of correlation of burnup measurements for physics prediction of fast power-reactor life. Nucl Sci Eng. 1969; 38: 1-7.

[2] Williams ML. Development of depletion perturbation theory for coupled neutron/nuclide fields. Nucl Sci Eng. 1979; 70: 20-36.

[3] Takeda T, Umano T. Burnup sensitivity analysis in a fast breeder reactor part I: sensitivity calculation method with generalized perturbation theory. Nucl Sci Eng. 1985; 91: 1-10.

[4] Yang WS, Downar TJ. Generalized perturbation theory for constant power core depletion. Nucl Sci Eng. 1988; 99: 353-366.

[5] Chiba G, Kawamoto Y, Narabayashi T. Development of a fuel depletion sensitivity calculation module for multi-cell problem in a deterministic reactor physics code system CBZ. Ann Nucl Energy. 2016; 96: 277-286.

[6] Stamm'ler RJJ, Abbate MJ. Methods of steady-state reactor physics in nuclear design. London: Academic Press; 1983.

[7] Okumura S, Chiba G. Development of nuclear fuel depletion calculation capability for LWR fuel assembly in reactor physics code system CBZ. Proc. Reactor Physics Asia 2017; 2017 Aug 24-25; Chengdu (China).

[8] Chiba G, Narabayashi T. Advanced Bondarenko method for resonance self-shielding calculations in deterministic reactor physics code system CBZ. Ann Nucl Energy. 2016; 96: 277-286.

[9] van Rooijen WFG, Chiba G. Diffusion coefficients for LMFBR cells calculated with MOC and Monte Carlo methods. Ann Nucl Energy. 2011; 38: 133-144.

[10] Kawamoto Y, Chiba G, Tsuji M, Narabayashi T. Numerical solution of matrix exponential in burn-up equation using mini-max polynomial approximation. Ann Nucl Energy. 2015; 80: 219-224.

[11] Chiba G, Tsuji M, Narabayashi T. Uncertainty quantification of neutronic parameters of light water reactor fuel cells with JENDL-4.0 covariance data. J Nucl Sci Technol. 2013; 50: 751-760.

[12] Katakura J, Kataoka M, Suyama K, Jin T, Ohki S. A set of ORIGEN2 cross section libraries based

on JENDL-3.3 library: ORLIBJ33. Japan: Japan Atomic Energy Research Institute; 2004, JAERI-Data/Code 2004-015.[in Japanese]

[13] Chiba G, Tsuji M, Narabayashi T, Ohoka Y, Ushio T. Important fission product nuclides identification method for simplified burnup chain construction, J Nucl Sci Technol. 2015; 52: 953-960.

Figure Captions

Figure 1 Geometric configuration of a 3×3 multicell system including gadolinium-bearing UO_2 fuel pin.

Figure 2 Infinite neutron multiplication factors with fuel depletion.

Figure 3 Sensitivities of gadolinium-157 number density at peripheral region of pin 1 at 9.6 GWD/t

Figure 4 Sensitivities of gadolinium-157 number density at center region of pin 1 at 20.8 GWD/t

Figure 5 Sensitivities of number densities at pin 2 at 20.8 GWD/t with respect to gadolinium-157 capture cross sections

Figure 6 Sensitivities of gadolinium-157 number density at center region of pin 1 at 9.6 GWD/t with respect to uranium-235 fission cross section

Figure 7 Sensitivities of gadolinium-157 number density at center region of pin 1 at 9.6 GWD/t with respect to uranium-238 capture cross section

Figure 8 Sensitivities of gadolinium-155 number density at center region of pin 1 at 9.6 GWD/t with respect to uranium-235 fission cross section

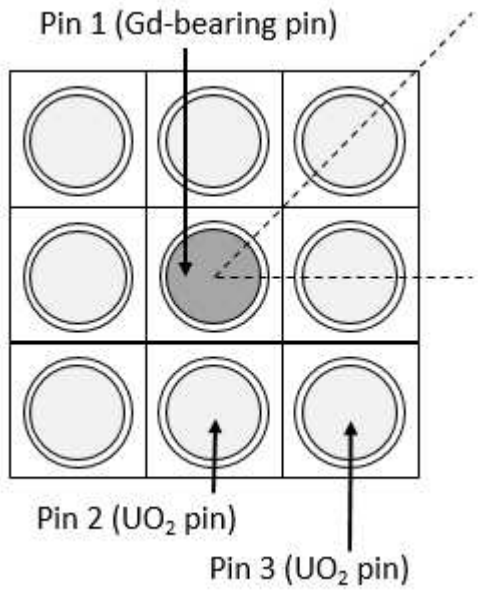

Figure 1 Geometric configuration of a 3×3 multicell system including gadolinium-bearing UO_2 fuel pin.

G.Chiba

Perturbation theory for nuclear fuel depletion calculations with predictor-corrector method

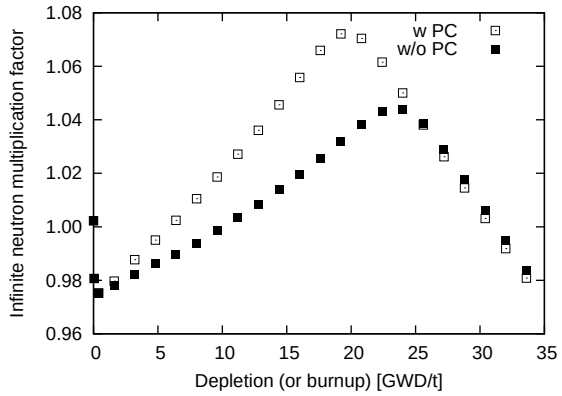

Figure 2 Infinite neutron multiplication factors with fuel depletion.

G.Chiba

Perturbation theory for nuclear fuel depletion calculations with predictor-corrector method

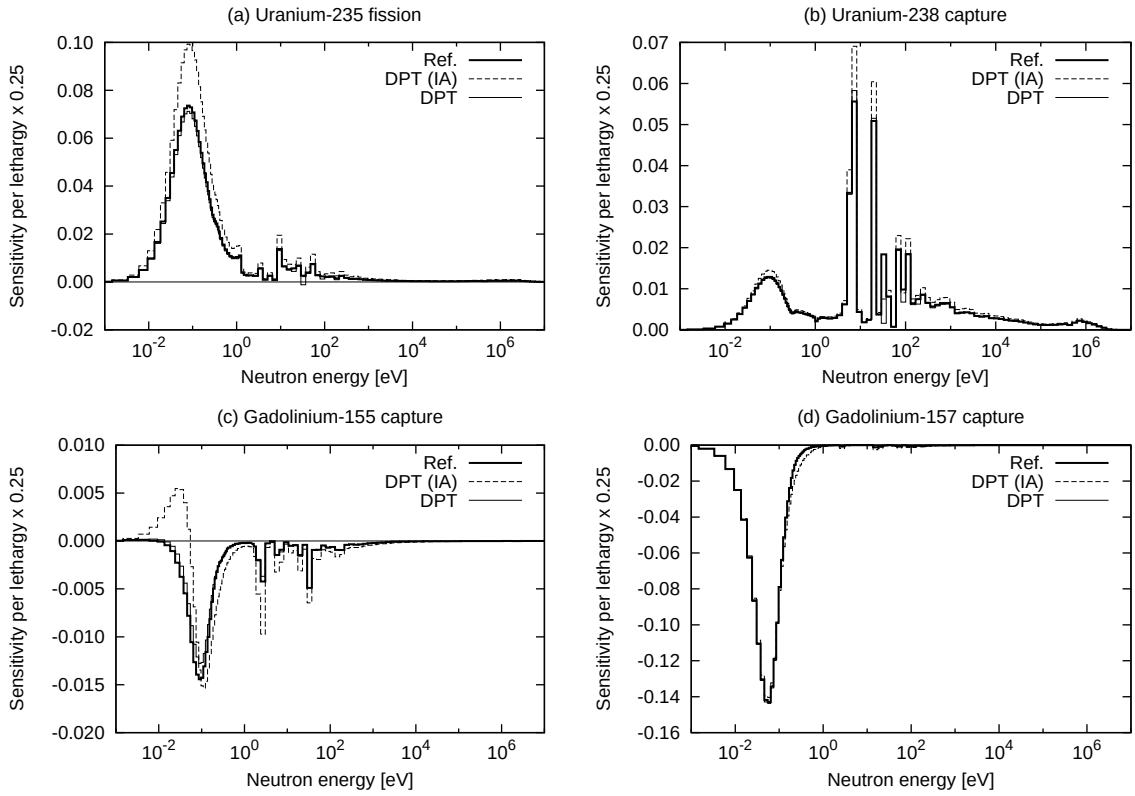

Figure 3 Sensitivities of gadolinium-157 number density at peripheral region of pin 1 at 9.6 GWD/t

G.Chiba

Perturbation theory for nuclear fuel depletion calculations with predictor-corrector method

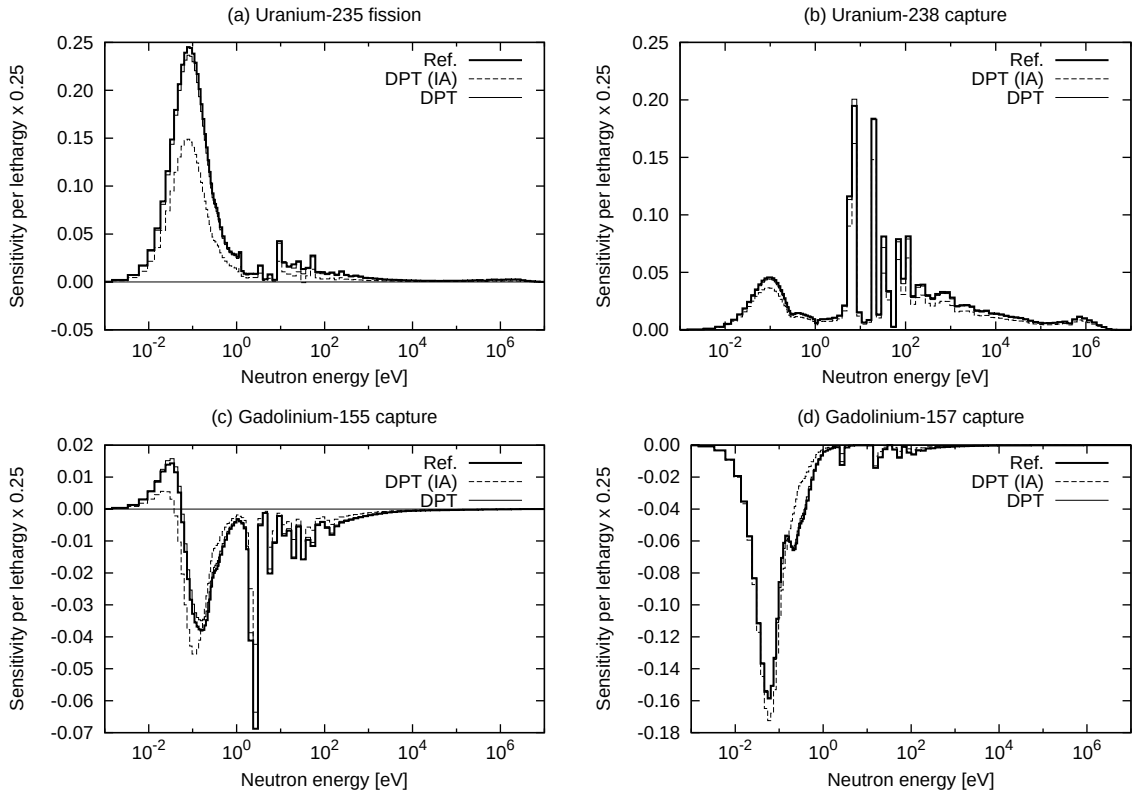

Figure 4 Sensitivities of gadolinium-157 number density at center region of pin 1 at 20.8 GWD/t

G.Chiba

Perturbation theory for nuclear fuel depletion calculations with predictor-corrector method

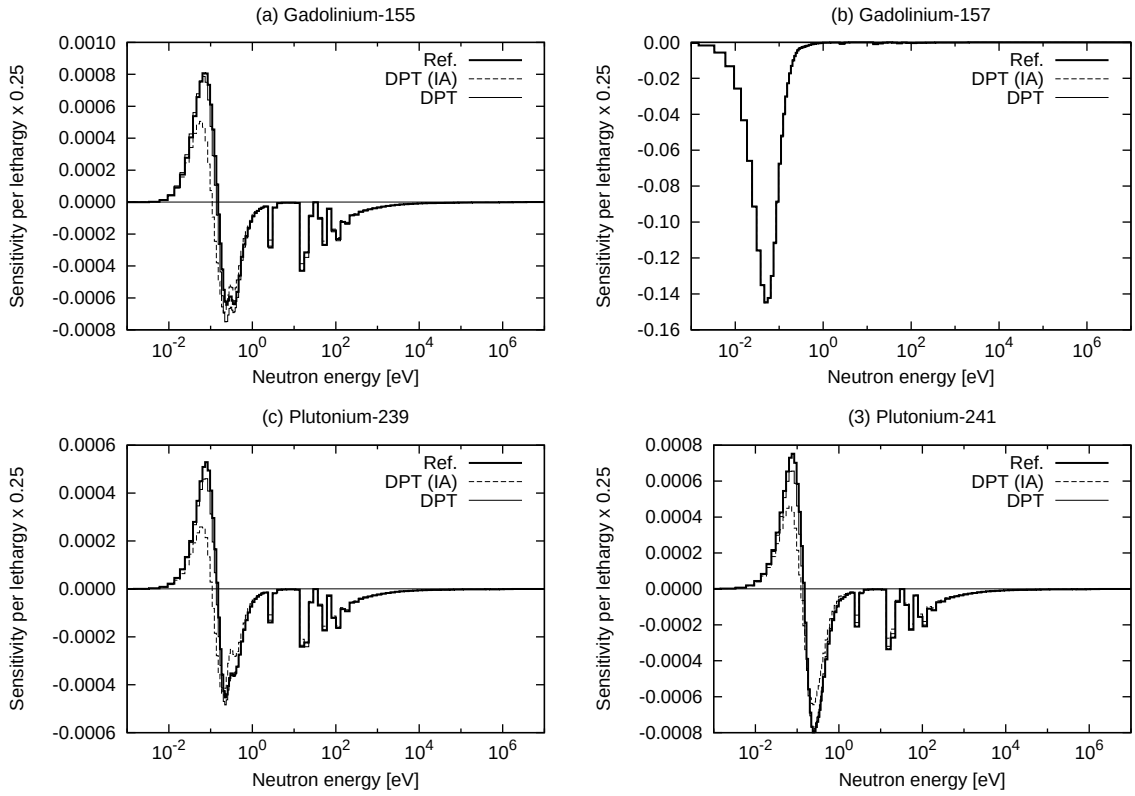

Figure 5 Sensitivities of number densities at pin 2 at 20.8 GWD/t with respect to gadolinium-157 capture cross sections

G.Chiba

Perturbation theory for nuclear fuel depletion calculations with predictor-corrector method

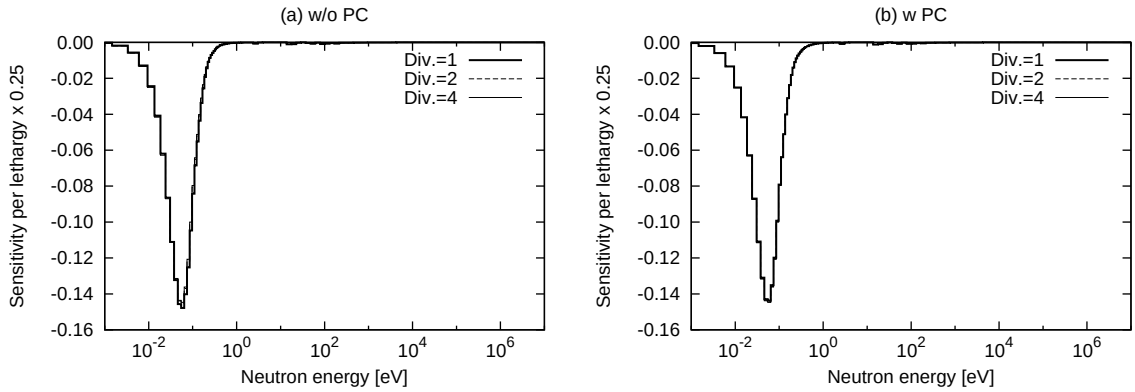

Figure 6 Sensitivities of gadolinium-157 number density at center region of pin 1 at 9.6 GWD/t with respect to uranium-235 fission cross section

G.Chiba

Perturbation theory for nuclear fuel depletion calculations with predictor-corrector method

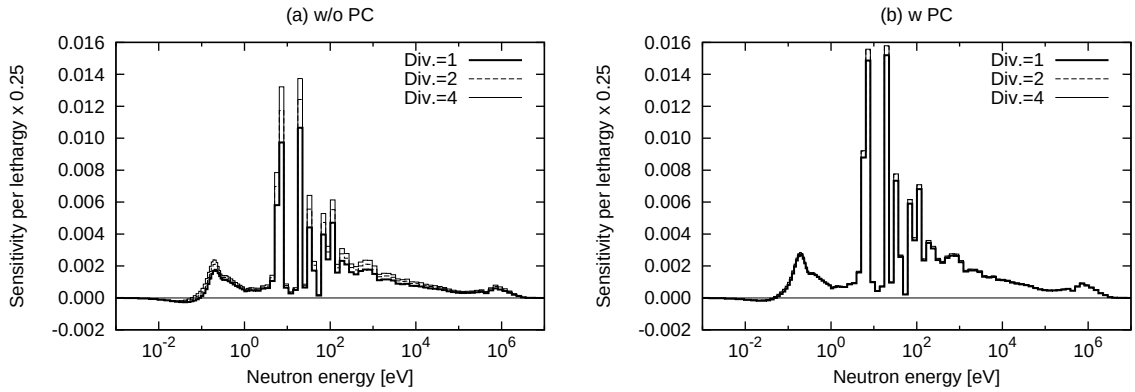

Figure 7 Sensitivities of gadolinium-157 number density at center region of pin 1 at 9.6 GWD/t with respect to uranium-238 capture cross section

G.Chiba

Perturbation theory for nuclear fuel depletion calculations with predictor-corrector method

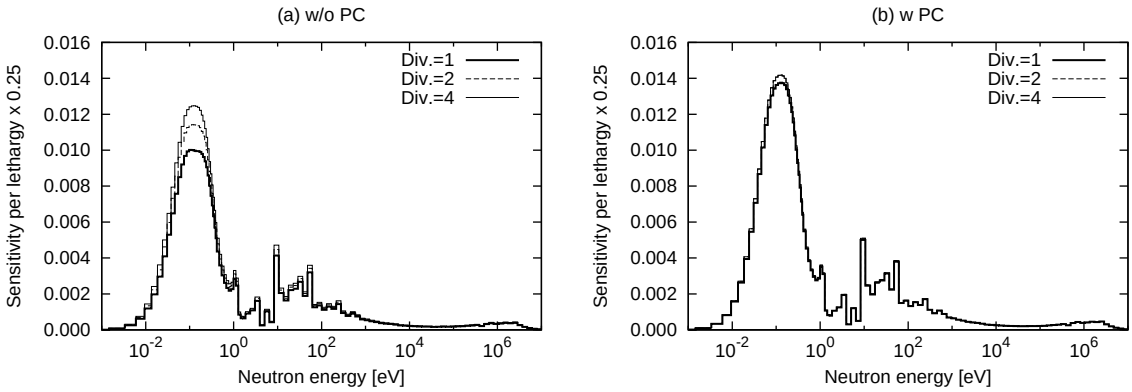

Figure 8 Sensitivities of gadolinium-155 number density at center region of pin 1 at 9.6 GWD/t with respect to uranium-235 fission cross section

G.Chiba

Perturbation theory for nuclear fuel depletion calculations with predictor-corrector method